NASA/TM—2018-219868

Optical Spectra of Lunar Dust Simulants

James R. Gaier
Glenn Research Center, Cleveland, Ohio

May 2018

NASA STI Program . . . in Profile

Since its founding, NASA has been dedicated to the advancement of aeronautics and space science. The NASA Scientific and Technical Information (STI) Program plays a key part in helping NASA maintain this important role.

The NASA STI Program operates under the auspices of the Agency Chief Information Officer. It collects, organizes, provides for archiving, and disseminates NASA's STI. The NASA STI Program provides access to the NASA Technical Report Server—Registered (NTRS Reg) and NASA Technical Report Server—Public (NTRS) thus providing one of the largest collections of aeronautical and space science STI in the world. Results are published in both non-NASA channels and by NASA in the NASA STI Report Series, which includes the following report types:

- TECHNICAL PUBLICATION. Reports of completed research or a major significant phase of research that present the results of NASA programs and include extensive data or theoretical analysis. Includes compilations of significant scientific and technical data and information deemed to be of continuing reference value. NASA counter-part of peer-reviewed formal professional papers, but has less stringent limitations on manuscript length and extent of graphic presentations.

- TECHNICAL MEMORANDUM. Scientific and technical findings that are preliminary or of specialized interest, e.g., "quick-release" reports, working papers, and bibliographies that contain minimal annotation. Does not contain extensive analysis.

- CONTRACTOR REPORT. Scientific and technical findings by NASA-sponsored contractors and grantees.

- CONFERENCE PUBLICATION. Collected papers from scientific and technical conferences, symposia, seminars, or other meetings sponsored or co-sponsored by NASA.

- SPECIAL PUBLICATION. Scientific, technical, or historical information from NASA programs, projects, and missions, often concerned with subjects having substantial public interest.

- TECHNICAL TRANSLATION. English-language translations of foreign scientific and technical material pertinent to NASA's mission.

For more information about the NASA STI program, see the following:

- Access the NASA STI program home page at http://www.sti.nasa.gov

- E-mail your question to help@sti.nasa.gov

- Fax your question to the NASA STI Information Desk at 757-864-6500

- Telephone the NASA STI Information Desk at 757-864-9658

- Write to:
  NASA STI Program
  Mail Stop 148
  NASA Langley Research Center
  Hampton, VA 23681-2199

NASA/TM—2018-219868

Optical Spectra of Lunar Dust Simulants

James R. Gaier
Glenn Research Center, Cleveland, Ohio

National Aeronautics and
Space Administration

Glenn Research Center
Cleveland, Ohio 44135

May 2018

Acknowledgments

The author gladly acknowledges the contributions of K.W. Street, S.K.R. Miller, and D.A. Jaworske of the NASA Glenn Research Center, and Lewis' Educational and Research Collaborative Internship Project (LeRCIP) Interns S. Ellis and N. Hanks for assistance with the spectroscopy, and D.L. Rickman of the NASA Marshall Spaceflight Center, and D.B. Stoesser and S.A. Wilson of the U.S. Geological Survey for their many helpful discussions about the properties of the lunar regolith and lunar simulants. R.J. Gustafson of Orbital Technologies kindly provided simulant samples. Programmatic and financial support from the NASA Exploration Technology Development Program came through the Dust Mitigation Project (M.J. Hyatt at the NASA Glenn Research Center) and the Advanced Thermal Control Project (R.A. Stephan, NASA Johnson Space Center.)

Level of Review: This material has been technically reviewed by technical management.

Available from

NASA STI Program
Mail Stop 148
NASA Langley Research Center
Hampton, VA 23681-2199

National Technical Information Service
5285 Port Royal Road
Springfield, VA 22161
703-605-6000

This report is available in electronic form at http://www.sti.nasa.gov/ and http://ntrs.nasa.gov/

Optical Spectra of Lunar Dust Simulants

James R. Gaier
National Aeronautics and Space Administration
Glenn Research Center
Cleveland, Ohio 44135

Abstract

A comparative study of the reflectance spectra of lunar dust simulants is presented. All of the simulants except one had a wavelength-dependent reflectivity ($\rho(\lambda)$) near 0.16 over the wavelength range of 8 to 25 μm, so they are highly emitting at room temperature and lower. The 300 K emittance (ε) of all the lunar simulants except MLS–1 ranged from 0.82 to 0.86. There was considerably more variation in the lunar simulant reflectance in the solar spectral range (250 to 2,500 nm) than in the thermal infrared. As expected, the lunar highlands simulants were more reflective in this wavelength range than the lunar mare simulants. The integrated solar absorptance (α) of the simulants ranged from 0.42 to 0.81. Although large spectral differences between simulant dusts and actual reported lunar dusts were observed, the integrated α of JSC–1AF and MLS–1P is similar to that of mare dusts, and FJS–1 and the JSC–1 have integrated α that match the highland dust quite well.

Introduction

As NASA prepares to return humans to the Moon, extensive efforts are under way to design the thermal control systems that will protect future lunar landers and surface system elements from the harsh lunar thermal environment. Part of this effort is to determine the effects of dust deposited on the thermal control surfaces. But even a casual glance up at the Moon reveals that the lunar surface is not uniform in brightness. The albedo of specific areas of the Moon varies from 0.50 for the brightest features to 0.07 for the darkest (Ref. 1). If the dust is darker, then more light will be absorbed by it, resulting in increased heating both of the dust and, through conduction and radiation, any thermal control surface it may land on. To quantify these effects, lunar simulants must be developed that have a variety of reflectance properties.

But there are several characteristics of the albedo which limit its usefulness when assessing the effects of radiant energy on thermal control systems. First, as these measurements are typically made from either from earth-based instruments or from lunar orbit, the topographical features within the measurement frame will affect the measurement. Any shadowed areas will skew the albedo to a lower value. And even for those areas lit, the fraction of light reflected is dependent on the angle of incidence. The bidirectional reflectance function of the lunar surfaces is known to be decidedly non-Lambertian. In addition, the albedo is typically measured in the visible region of the spectrum (400 to 700 nm wavelength), and the solar radiation is principally emitted over a wider spectral region, 250 to 2,500 nm (Figure 1).

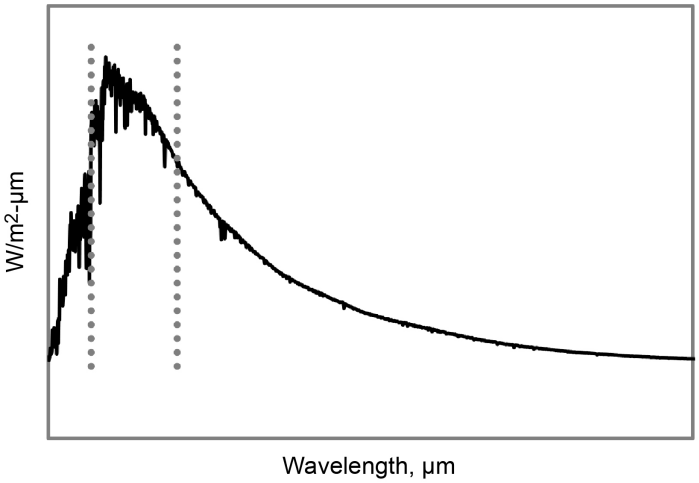

Figure 1.—The solar spectrum measured at 1 AU from the Sun above the Earth's atmosphere (Air Mass Zero spectrum) (Ref. 11). The visible spectrum is the region between the dotted lines.

More useful measures for most analyses are intrinsic material properties such as the wavelength dependant absorptivity ($\alpha(\lambda)$), reflectivity ($\rho(\lambda)$), and transmissivity ($T(\lambda)$). These three properties are related through conservation of energy, since a photon must either be absorbed, reflected, or transmitted as described by the equation:

$$\alpha(\lambda) + \rho(\lambda) + T(\lambda) = 1 \tag{1}$$

Under the usual condition for the lunar surface where the surface is opaque ($T = 0$), Equation (1) reduces to:

$$\alpha(\lambda) = 1 - \rho(\lambda) \tag{2}$$

A further useful relationship is Kirchhoff's Law, which states that for a given wavelength of light the emissivity ($\varepsilon(\lambda)$) of a surface is equal to its $\alpha(\lambda)$, or:

$$\varepsilon(\lambda) = \alpha(\lambda) \tag{3}$$

In thermal analysis the quantity usually required is the total integrated absorptance (α) and total integrated emittance (ε). As illustrated in Figure 1, convolving the $\alpha(\lambda)$ of a material over the 250 to 2,500 nm range with the air mass zero (AM0) solar spectrum yields a very good approximation of α, since there is little solar intensity outside this spectral range.

The intensity of $\varepsilon(\lambda)$ is temperature dependant. The temperature ranges of interest range from the hottest surfaces of a nuclear reactor (perhaps 800 K) to the coldest of the permanently shadowed craters (perhaps 25 K), though the daily lunar temperature swing of 100 to 400 K will encompass most scenarios. The relationship between wavelength and temperature can be approximated by the Raleigh-Jeans law, which determines the wavelength at which the intensity for a blackbody radiation curve at a given temperature is maximum. Temperatures of interest and their corresponding wavelengths are shown in Table 1.

TABLE 1.—TEMPERATURES OF INTEREST AND THEIR CORRESPONDING WAVELENGTHS ACCORDING TO THE RALEIGH-JEANS LAW

Feature	Temperature, K	Wavelength max, μm
Permanently shadowed craters	25	115
Lunar night	100	29
Lunar polar regions	200	14
Lunar habitat temperature	300	10
Lunar equator at noon	400	7
Nuclear reactor radiator	800	4

As evidenced in this volume, lunar simulant development is a rapidly evolving field. Although thermal optical properties of the lunar regolith are critical to designing systems that will survive the challenging lunar thermal environment, there has been very little work to characterize the properties of lunar simulants. The reflectance spectra in the 250 nm to 25 μm range, the integrated solar α, and the 300 K ε values will be reported for a variety of lunar simulants.

Methods and Materials

Spectroscopic Methods

In order to determine the α of a simulant powder, the $\alpha(\lambda)$ over the solar spectrum must be determined. The easiest way to do that is to measure its $\rho(\lambda)$ and apply Equation (2). Since on the lunar surface sunlight will impinge on the dust particles both directly and from many different reflected directions, the total $\rho(\lambda)$, including the specular and diffuse components is the quantity of interest. This is best accomplished using a spectrophotometer equipped with an integrating sphere. The reflectance spectra reported here were collected on a Cary 5000 spectrophotometer (Varian) equipped with a DRA 2500, 150 mm diameter integrating sphere over the wavelength range of 250 to 2,500 nm.

Great care must also be taken in the preparation of the sample. How tightly the powder is packed will make a difference in this wavelength range, with lose powders reflecting less. In this study a Varian powder attachment was used. A sample is trapped in a compression cell, one side of which is a quartz window. The cell is tightened to the point where the powder makes a smooth and uniform surface, and the grains do not move when the cell is tipped or rotated. The Varian powder attachment was filled with 10 grams of sample which resulted in a sample about 4 mm thick, too thick for transmittance.

Determining the scale factors to put the $\rho(\lambda)$ measurement on an absolute scale must be done thoughtfully as well. The 100 percent reflectance must be set with a powdered standard, which in turn must be calibrated against a NIST-traceable standard. Ideally, this calibration should be against a suite of NIST-traceable standards of varying $\rho(\lambda)$ to determine the response function of the detector. In this study a second, manufacture-provided powder attachment filled with powdered Spectralon®, the same material that coated the inside of the integrating sphere, and a quartz window matched with the sample holder was used for the baseline. A set of eight NIST traceable diffuse reflectance standards (Labsphere) with ρ ranging from 0.02 to 0.99 was measured through the quartz window as well. An intensity dependent correction factor was applied to the averaged ρ for each sample to place it on an absolute scale.

Data were collected from 250 to 2,500 nm in increments of 1 nm, at a scan rate of 600 nm/min. A deuterium lamp was used to measure the 250 to 350 nm data, and a halogen lamp to measure the 350 to 2,500 nm data. Immediately prior to running each sample, a spectrum of the Spectralon® was collected as a sample, to determine whether the baseline was still valid. In all instances the deviations in the baseline were less than 1 percent. Three spectra of each sample were collected consecutively. The sample holder was rotated between each spectrum so that the beam sampled a different area of the sample. If the three spectra were determined to be similar enough, the three spectra were averaged, point by point, and multiplied by the ratio of blank to baseline.

The integrated solar α of each sample was determined by calculating the convolution of the scaled $\rho(\lambda)$ of the simulant with the ASTM AM0 solar spectrum E–490–00 and expressed as a fraction of the solar spectrum.

In order to determine the thermal ε, a similar procedure is required but in the thermal infrared part of the spectrum. The $\varepsilon(\lambda)$ is determined from the $\alpha(\lambda)$ using Equation (3), which is in turn determined from the $\rho(\lambda)$ using Equation (2). Ideally the thermal infrared $\rho(\lambda)$ spectra should overlap with the solar $\rho(\lambda)$ spectrum (i.e., stating at less than 2.5 μm) and extend up to the wavelength that corresponds to the lowest temperature expected (i.e., 115 μm). But due to practical instrument considerations, it is difficult to measure infrared $\rho(\lambda)$ at wavelengths longer than about 25 μm.

Ambient laboratory air contains enough of carbon dioxide and water to absorb the infrared in the light path, and distort the $\rho(\lambda)$ spectrum. So the integrating sphere was flooded with dry nitrogen to reduce absorption enough that the $\rho(\lambda)$ signal of the simulant can dominate. For this study reflectance spectra in the 2.5 to 25 μm range were collected on a Magna-IR 760 (Nicolet) equipped with a Labsphere RSA–NI–550ID 76 mm Infragold® integrating sphere using a deuterated triglycidyl sulfate detector. This is a Fourier transform instrument and 100 scans with a data point spacing of 7.714 cm^{-1} were collected for each sample. A gold background spectrum was measured prior to each scan. The integrating sphere was purged with dry nitrogen to eliminate background water and carbon dioxide bands. Powder samples of 4 to 6 mm thickness were placed in a Fluoroware dish which was placed at the sample port at the bottom of the integrating sphere. No window was necessary in this configuration. None of the Fluoroware spectral peaks were visible in any of the spectra, indicating that the samples were optically opaque. During the course of the data collection two NIST traceable standards of similar reflectivity (SRS–10–010 and SRS–20–010) were measured as well.

There are subtle differences between the ways the data were collected on the two spectrophotometers. In the Cary, the sample was physically substituted for the reference on the surface of the integrating sphere. But in the Nicolet, the sample was measured by alternating a mirror between positions where the reference was measured, or the sample was measured. So in the case of the Nicolet, some small fraction of the integrating sphere when the reference is being measured is covered with the sample, whereas in the Cary it is not. This correction factor is dependent on the reflectance of the sample.

The integrated thermal ε should be determined at least over the full temperature range expected on the lunar surface, 100 to 400 K. This was calculated by convoluting the 2.5 to 25 μm wavelength $\varepsilon(\lambda)$ data with blackbody curves over the temperature range in 5 K increments (Ref. 2).

Lunar Simulants

The basic spectra of five lunar simulants of the most common were measured, three mare type and two highlands type. The first of these basic four is JSC–1A, a mare-type simulant that is a remake of the JSC–1 simulant that has been the *de facto* NASA simulant since it was introduced in 1994 (Ref. 3). The second was a simulant developed by researchers at the University of Minnesota in 1988 approximating the bulk chemistry of Apollo 11 soil sample 10084, Minnesota Lunar Simulant 1 (MLS–1) (Ref. 4). The third was developed in Japan in 1995 from the volcanic soils on Fujisan called FJS–1 (Ref. 5). The fourth was a lunar highlands type simulant produced through a current joint effort of NASA and the U.S. Geological Survey, NU–LHT–2M (Ref. 6). The recently developed Canadian highlands simulant Chenobi, was tested as well (Ref. 7).

In addition to those simulants, four simulant variants were measured to determine the general effects of adding minor constituents to the simulants. Since JSC–1A is a remake of JSC–1, their spectra should be identical. This was examined. MLS–1P is a variant of MLS–1 produced by dropping the MLS–1 through a 6,000 °C plasma in an in-flight sustained shockwave plasma reactor, 10 m tall. MLS–1 itself has essentially no glass content, but glass content from 10 to 30 percent was achieved with feed rates of 40 to 50 kg/hr. Although no agglutinate-like materials were produced, part of the simulant was melted into glassy spheroids, some as large as 2 mm. ORBITEC, under a Phase I SBIR contract, used a

proprietary process to create a mature lunar regolith simulant designated JSC–1A–5000–2X that contains a high proportion of agglutinate-like particles and glass spherules, both of which contain metallic iron globules (including nanophase Fe^0). They also processed NU–LHT–2M in a similar manner to create a highlands simulant, designated NU–LHT–2M–700–1X containing simulated agglutinates with iron globules (Ref. 8).

Processing the Lunar Simulants

Particle size is known to affect the $\rho(\lambda)$ of powdered rock and mineral samples. This was dramatically shown in the case of lunar regolith in the data reported by the Lunar Soil Characterization Consortium, who measured the $\rho(\lambda)$ of sieved fractions of lunar samples returned during Apollo (Ref. 9). They found that smaller particles were both more reflective and showed fewer spectral features. Since the simulants were acquired with a wide variety of particle sizes, they were processed to remove particle size as an important factor. In order to determine the reflectance of the dust fraction of the simulants, each was dry ground in a micronizing vibratory mill (McCrone Scientific, Ltd., London) for 90 min, and then sieved through a 20 μm sieve (No 450). The dust is seen as the most important fraction to characterize, because these are the particles that will be most difficult to remove from exploration system hardware, including thermal control surfaces.

Grinding the simulants to decrease their particle size has consequences for both their solar optical and thermal optical spectra. In Figure 2(a) the $\rho(\lambda)$ of JSC–1A–5000–2X ground and sieved to 20 μm is compared to the same simulant ground to 10 μm over the 250 to 2,500 nm range. The 10 μm is lighter, with the longer wavelength portion of the spectrum being more affected. In all cases the simulants became more reflective in this spectral region as the material was more finely ground. Usually the difference is visible to the unaided eye. A different effect is illustrated in Figure 2(b), which shows the spectra in the thermal infrared range of MLS–1 before and after grinding. In this case, decreasing the particle size decreases the $\rho(\lambda)$. The initial MLS–1 was very crystalline with virtually no glassy particles in it. As the particles were ground the glass content increased, which increases the absorption in this part of the spectrum. The higher reflectivity of smaller particles and the mechanically induced glassification on grinding are two important effects to remember when the spectra of dust particles are compared to those of simulants with larger particle size.

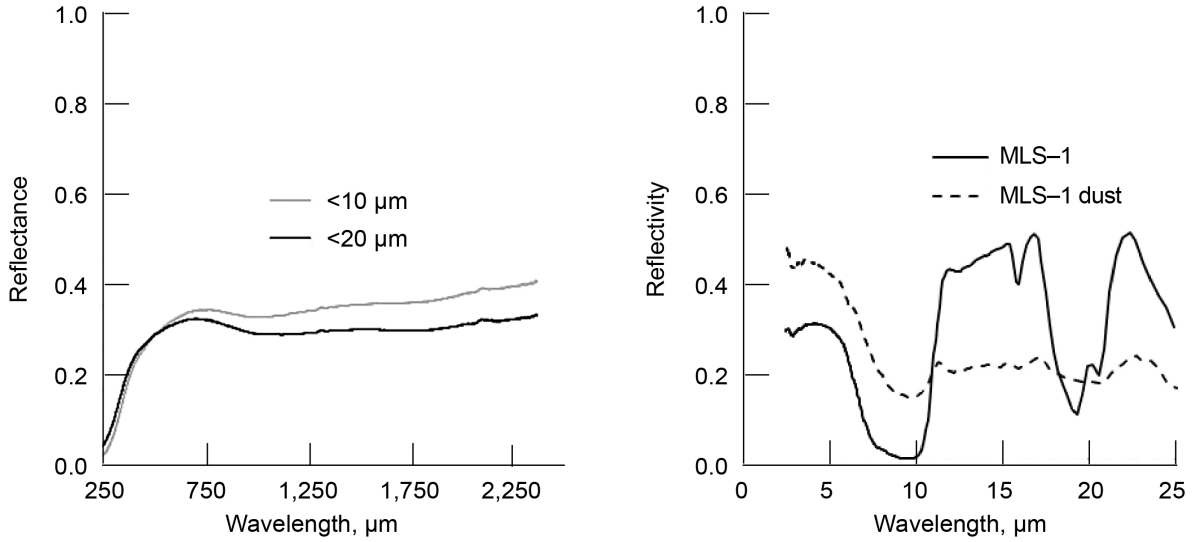

Figure 2.—Total reflectance spectra of the JSC–1A–5000–2X ground and sieved to two different particle sizes in the solar spectral region (a). Total reflectance spectra of MLS-1 before and after grinding and sieving in the thermal emittance spectral region (b).

Results and Discussion

Reflectivity Measurements

Figure 3 shows bidirectional reflectance spectra measured of a mare soil (12001) and a highlands soil (64801) returned by Apollo 12 and 16, respectively as reported by the Lunar Soil Characterization Consortium on their website (Ref. 12). Note that, as seen in the samples in this study, the $\rho(\lambda)$ increases as the particle size decreases. This is attributed, at least in part, to their observation that the finer fraction contains more feldspar, which is lighter in color than the more mafic pyroxenes. The composition of the simulants, however, is nearly invariant between the larger and smaller components because the fine fractions are produced from grinding the coarser fractions. The reflectance of the lunar samples rises nearly monotonically throughout the 300 to 2,600 nm range. But in all cases the simulant reflectivity rises sharply over the 250 to 500 nm range, and then are nearly invariant through 2,500 nm. (The peak observed in the 1900 to 2,200 region is associated with the quartz window.) So if the spectral details of reflection are important to an application in the solar absorption region, none of the current simulants are satisfactory.

The reflectance spectra of Chenobi, NU–LHT–2M, MLS–1, JSC–1A, and FJS–1, sieved to below 20 μm particles, are shown in Figure 3. Large differences are noted among the six basic simulants in the $\rho(\lambda)$ in the 250 to 2,500 nm range (Figure 4(a)), where the solar spectrum is the most intense. Even before a quantitative analysis, it is apparent from these spectra that there will be substantial variations in the solar α among the simulants. As expected, the two highlands type simulants, Chenobi and NU–LHT–2M are more reflective than the mare types.

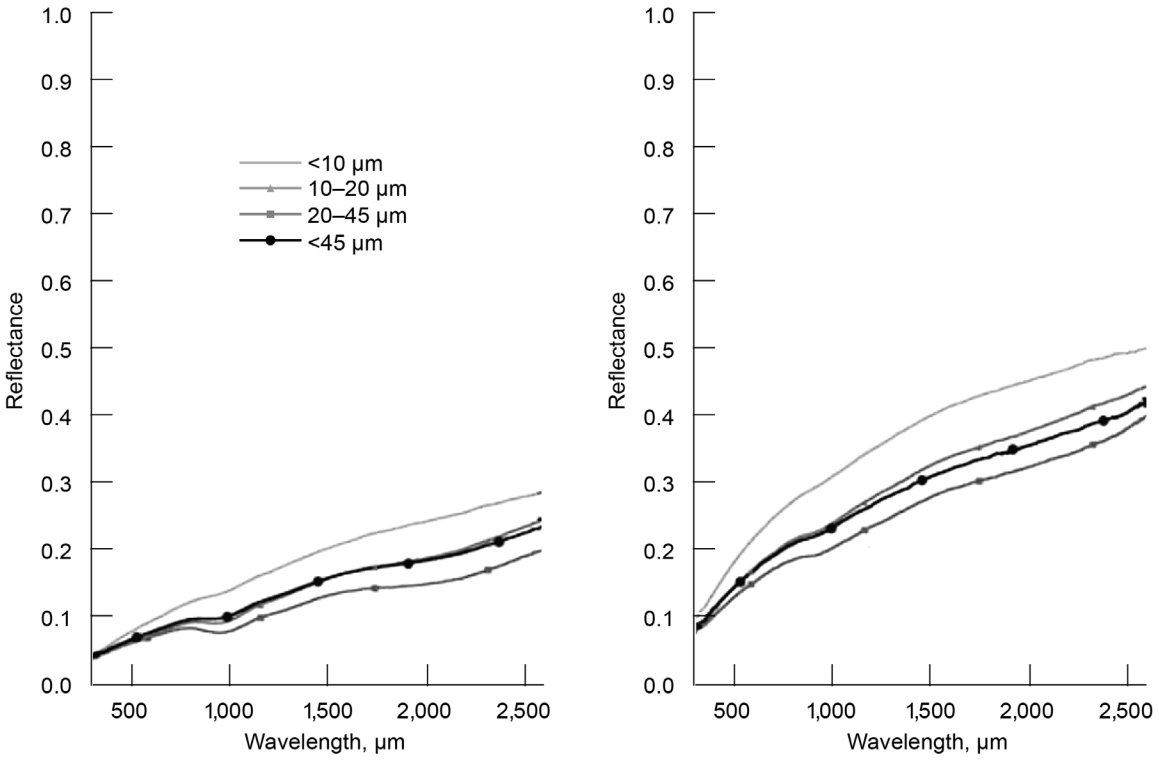

Figure 3.—The bidirectional reflectance spectra (a) Apollo 12001 mare and (b) Apollo 64801 highland lunar soils (Ref. 9).

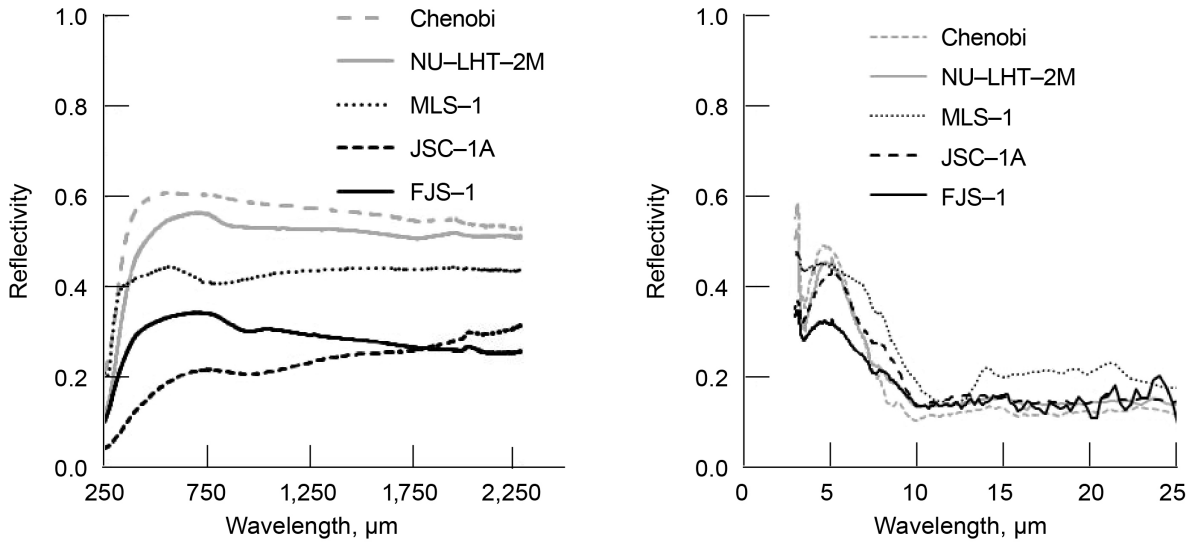

Figure 4.—Reflectance spectra of the six baseline simulants measured in this study in the solar absorptance region (a), and for the thermal emittance region (b).

It is clear from Figure 3(b) that there is little difference in the $\rho(\lambda)$ among the simulants at wavelengths greater than about 8,000 nm, except for the case of MLS–1. Further, the infrared $\rho(\lambda)$ for those simulants is about 0.15 for wavelengths longer than 8,000 nm. Using the Raleigh-Jeans law this corresponds to temperature of 360 K and lower, so for the temperatures at which the thermal control surfaces are expected to operate under lunar conditions, the ε's are all about the same. This implies that the thermal emission properties all over the lunar surface are likely to be similar, and in the range of 0.85.

The participants at the Lunar Regolith Simulant Materials Workshop convened by NASA in 2005 agreed that engineering quantities lunar simulants would be required to support the NASA's Exploration program. Since quantities of the mare simulant JSC–1 were largely depleted, it was decided to recreate that simulant, with the designation JSC–1A. Although the goal was an exact reproduction of JSC–1, it can be seen in Figure 5(a) that the solar reflectance spectrum differs appreciably. This illustrates an important lesson about the variability of natural materials. Even if the source material is taken from the same region and processed using the same techniques, there will be differences. So too will it be on the Moon. It will be more useful to consider the range of material properties the lunar regolith will have than to try to duplicate exactly one particular sample. But note that in the thermal infrared region (Figure 5(b)) that the two spectra are very similar, illustrating once again that the thermal emission properties of lunar simulant materials do not differ greatly.

It can be seen in Figure 4(b) that MLS–1 is much more reflecting than the other simulants in the 10 to 25 μm wavelength range. This is thought to be because MLS–1 contains almost no glass or agglutinates. Glasses are known to dramatically increase absorption over crystalline materials in this portion of the spectrum. In addition, the other simulants all have high glass content, as does the lunar soil. So MLS–1 would probably not be a good simulant to use if the ε properties are important to the test. But MLS–1P is a variant of this material that has been exposed to a high temperature plasma, in which part of the MLS–1 is melted, and quickly cooled to increase its glass content. Figure 6 shows the darkening that this produces over the entire spectral range.

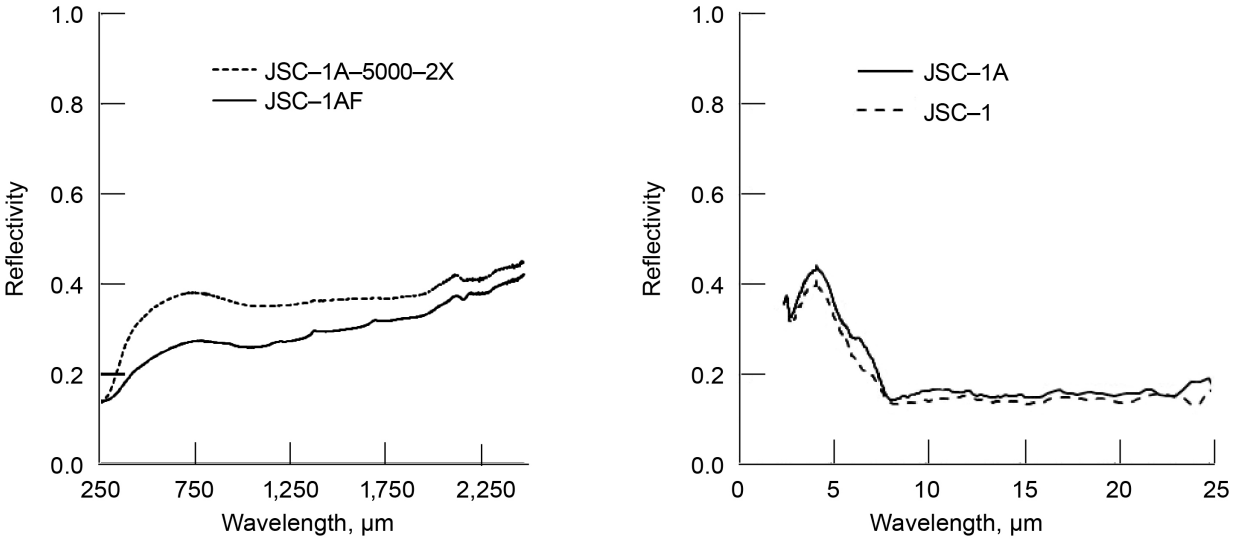

Figure 5.—Reflectance spectra of the JSC–1 and JSC–1A in the solar absorptance region (a), and for the thermal emittance region (b).

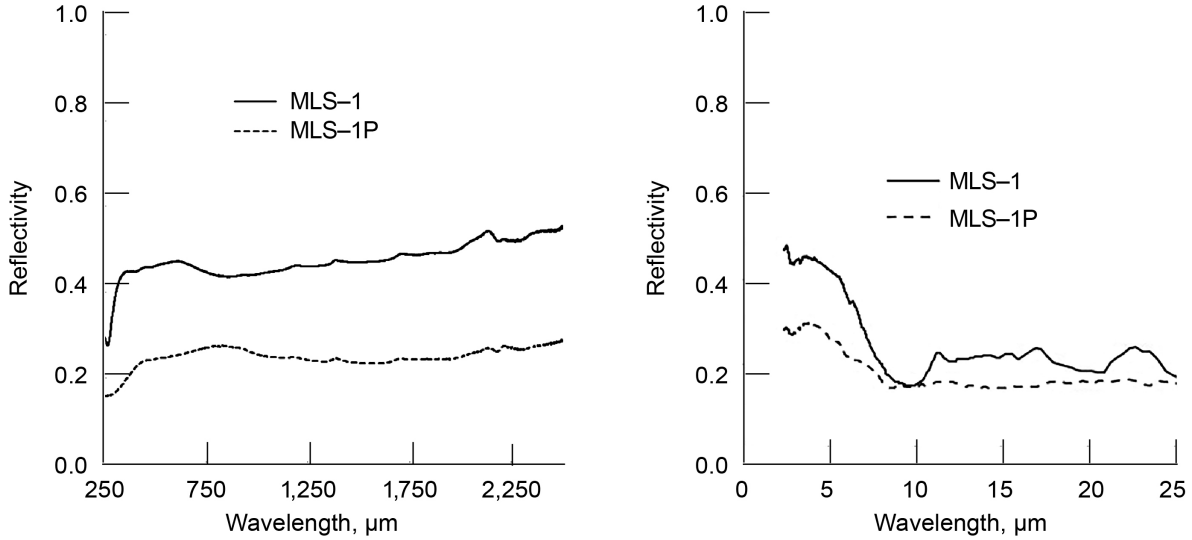

Figure 6.—Reflectance spectra of the MLS–1 and MLS–1P in the solar absorptance region (a), and for the thermal emittance region (b).

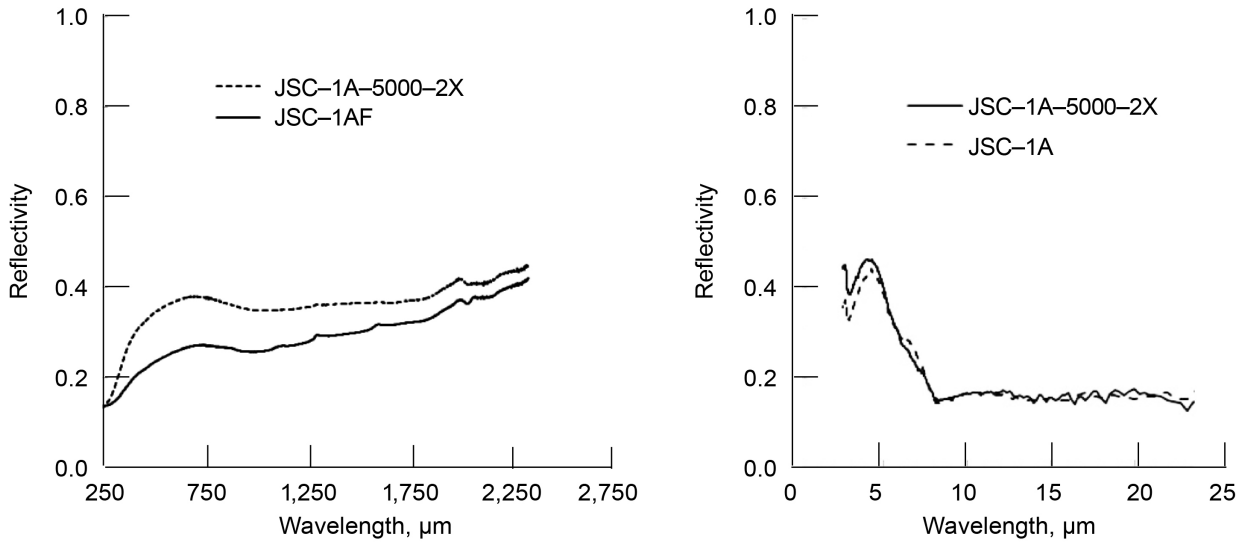

Figure 7.—Reflectance spectra of the JSC–1A and the synthetic agglutinate variant JSC–1A–5000–2X in the solar absorptance region (a), and for the thermal emittance region (b).

Unlike the lunar simulants in Figure 4(a), the $\rho(\lambda)$ of lunar soils increases almost monotonically over the range from 300 to 2,500 nm (Figure 3). This is often attributed to agglutinatic glass, and the nanophase iron it contains. So the addition of synthetic agglutinates, which also contain small metallic iron particles would be expected also to increase the $\rho(\lambda)$ over the base simulant in a similar way. Figure 7 shows $\rho(\lambda)$ for JSC–1A and its variant JSC–1A–5000–2X, which has synthetic agglutinate particles added to it. As with the previous cases there is much more variation in the 250 to 2,500 nm range (Figure 7(a)). However, the addition of the agglutinate glass after micronizing and sieving increases the reflectance of the samples rather than decreasing it. And even though the agglutinates contain iron-rich globules, there monotonically rising reflection spectrum of lunar dust samples was not in evidence. As before, there was little effect on the reflectivity in the thermal part of the spectrum (Figure 7(b)).

Figure 8 shows $\rho(\lambda)$ for NU–LHT and its variant NU–LHT–2M–700–1X which has agglutinates added using the same method as JSC–1A–5000–2X. Here, there was even a smaller effect of the synthetic agglutinates, if any at all, on the reflectance spectrum.

There are at least two possible explanations why the spectra of the simulants did not change as expected when the agglutinates were added. The first is that the synthetic agglutinates do not reproduce the key characteristics of the lunar agglutinates in sufficient fidelity. The most difficult part of the lunar agglutinate to reproduce is the nanophase iron which is found primarily in the amorphous “rind” around each grain, but also to a lesser extent on the grain surface. Even though nanophase iron has been observed in the transmission electron microscope, the particle size and distribution of the nanophase may be critical in some manner that is not as yet understood. The second explanation is that the effect in lunar materials may be cause by factors in addition to agglutinate and nanophase iron that are not as yet understood.

Like most lunar soils, the lunar simulants fall into two broad categories, the darker mare simulants and the lighter highlands simulants. In order to determine whether the effects on thermal control systems vary linearly with the darkness of the soil, a simulant of intermediate α was desired. To accomplish this, a 1:1 mixture of the light highlands simulant NU–LHT–1D and the dark mare simulant JSC–1AF was prepared. This also provided an opportunity to see how additive the α and ε of these multicomponent mixtures are. The results are shown in Figure 9, which shows the mixed simulant spectrum along with those of its constituents. Also shown is a point by point average of the two. It can be seen that the point-by-point average lies nearly on top of the 1:1 mixture, showing that the $\rho(\lambda)$ is rule-of-mixtures additive.

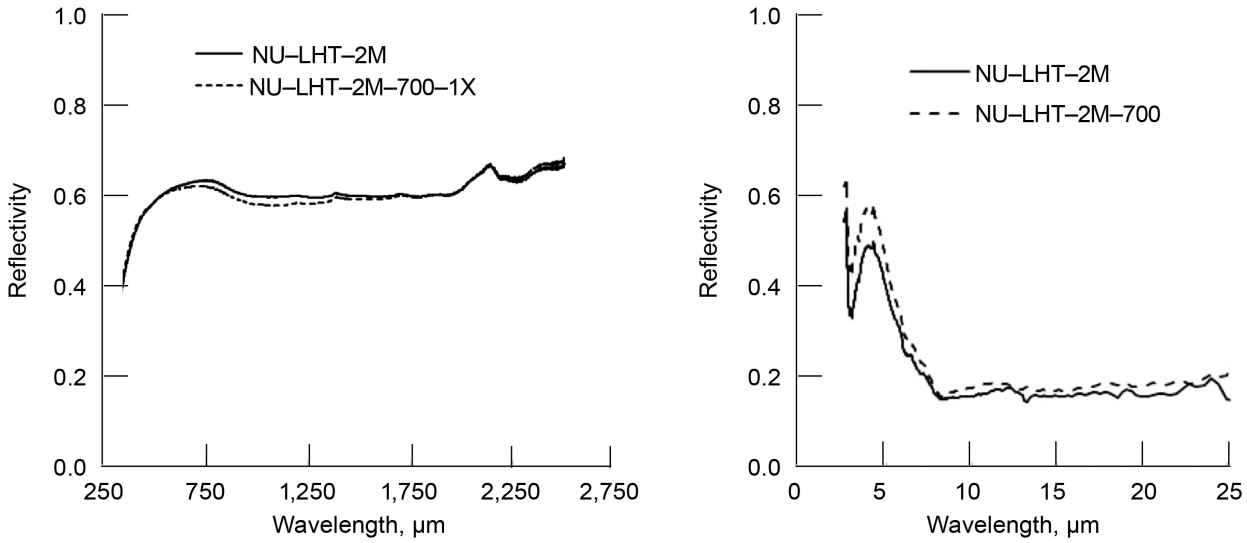

Figure 8.—Reflectance spectra of the NU–LHT–2M and the synthetic agglutinate variant NU–LHT–2M–700–1X in the solar absorptance region (a), and for the thermal emittance region (b).

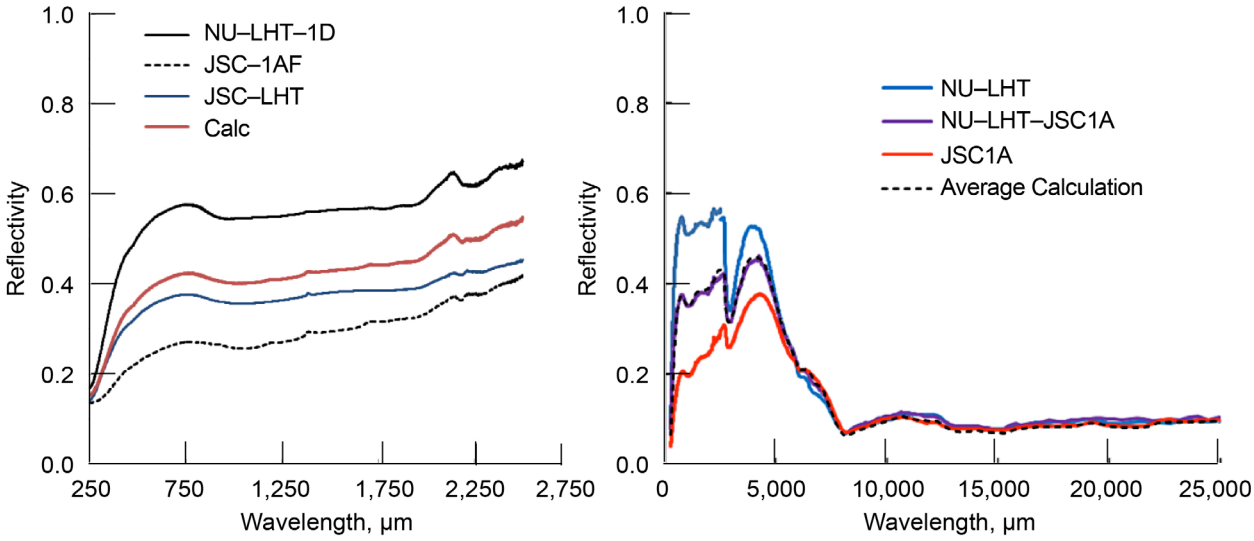

Figure 9.—The reflectance spectra of JSC–1AF, NU–LHT–1D and a 1:1 mixture of the two in the solar absorptance region (a), and for the absorptance and emittance regions (b). The dotted line shows the point by point average of JSC–1AF and NU–LHT–1D in the solar absorptance region (a), and for the absorptance and emittance regions (b).

Thermal Optical Property Calculations

Since the goal for this series of tests is to characterize the thermal properties of the simulant dust, the $\rho(\lambda)$ for each must be used to calculate the α and ε. The 250 to 2,500 nm data were used to calculate the α, and the 2.5 to 25 μm data to calculate the ε. The α and ε_{300} (ε at 300 K) for each of the simulants are listed in Table 2

The α ranged from 0.42 to 0.81 for the simulants. Albedo measurements suggest a range of α for the Moon of 0.50 to 0.93. As discussed above, the albedo measurements tend to indicate α values that are somewhat higher than expected from measuring the intrinsic α of the dust. In addition, these simulants would compare to the smallest fraction of the regolith, and for that reason would tend to be high. An appreciation for the size of the particle size effect for these materials can be gained by comparing these α values to those of the samples in their as-received sizes, as reported by Gaier, et al. (Ref. 10). Finally, the less than 20 μm fraction of the mare soil in Figure 3(a) has an $\alpha \approx 0.84$, which is higher than the average of 0.74 for the mare simulants tested here. However, JSC–1AF and MLS–1P both had $\alpha = 0.81$, and so would be reasonable simulants for integrated solar α. The α of the highland soils in Figure 3(b) has an $\alpha \approx 0.7$, which is considerably higher than the average of 0.5 for the mare simulants tested here. Some of the mare simulants such as FJS–1 and the JSC–1 have integrated α that match the highland dust quite well.

With the exception of MLS–1, the ε of all of the simulant dusts was 0.84±0.2. The ε at 300 K for each of the simulants is given in Table 2. If MLS–1 is excluded, the lunar simulants ε's range from 0.884 to 0.906 with an estimated error of ±0.005. This is not surprising when the $\rho(\lambda)$ of all of the simulants, except MLS–1, are essentially the same over the 8 to 25 μm wavelength range, all hovering around 0.10. The higher value for the $\rho(\lambda)$ in MLS–1 is probably due to the absence of glassy material, which are known to decrease the $\rho(\lambda)$ in the infrared. Since the lunar dust contains a very high fraction of impact glasses, the ε of the lunar dust would be expected to be high, and has been found to be about 0.95. The ε of the dust will also be somewhat higher than that of the thermal control surfaces, and so the blocking of emitted heat will probably not play a major role in thermal performance degradation. Nearly all of the dust degradation of thermal control surfaces will be due to increased α, that is, the dust will keep the solar incident light from reflecting off of the thermal control surface.

TABLE 2.—INTEGRATED SOLAR ABSORPTANCE (α) CALCULATED FROM 250 TO 2,500 nm TOTAL REFLECTIVITY AND INTEGRATED THERMAL EMITTANCE (ε) AT 300 K CALCULATED FROM 2.5 TO 25 μm TOTAL REFLECTIVITY

Simulant	Solar α	Thermal ε_{300}
Chenobi	0.42	0.86
NU–LHT–2M	0.49	0.84
NU–LHT–2M–700–1X	0.49	0.82
MLS–1	0.58	0.78
MLS–1P	0.81	0.84
JSC–1	0.71	0.84
JSC–1A	0.81	0.83
JSC–1A–5000–2X	0.67	0.83
FJS–1	0.69	0.84

Conclusions

A comparative study of the reflectance spectra of lunar dust simulants is presented. All of the simulants except one had a wavelength-dependent reflectivity ($\rho(\lambda)$) near 0.16 over the wavelength range of 8 to 25 μm, so they are highly emitting at room temperature and lower. The 300 K emittance (ε) of all the lunar simulants except MLS–1 ranged from 0.82 to 0.86. There was considerably more variation in the lunar simulant reflectance in the solar spectral range (250 to 2,500 nm) than in the thermal infrared. As expected, the lunar highlands simulants were more reflective in this wavelength range than the lunar mare simulants. The integrated solar absorptance (α) of the simulants ranged from 0.42 to 0.81. Although large spectral differences between simulant dusts and reported lunar dusts were observed, the integrated α of JSC–1AF and MLS–1P is similar to that of mare dusts, and FJS–1 and the JSC–1 have integrated α that match the highland dust quite well.

References

1. *Apollo 16 Preliminary Science Report*. NASA SP-31. (Brett R., England A.W., Calkins J.E., et al.). Washington, D.C.: NASA; 1972.
2. Jaworske D., Skowronski T. Portable Infrared Reflectometer for Evaluating Emittance. In: M.S. El-Genk *Space Technology and Applications Forum*. American Institute of Physics; 2000:CP-504.
3. McKay D., et al. JSC-1: A New Lunar Soil Simulant. In: *Engineering, Construction, and Operations in Space IV*. American Society of Civil Engineers; 1994:857–866.
4. Weiblen P., Gordon K. Characteristics of a Simulant for Lunar Surface Materials. In: *Second Conference on Lunar Bases and Space Activities in the 21st Century*. Lunar and Planetary Institute; 1988:652.
5. Kanamori H., et al. Properties of Lunar Soil Simulant Manufactured in Japan. In: *Proceedings of the 6th International Conference and Exposition on Engineering, Constructions, and Operations in Space*. Albuquerque: ASCE; 1998.
6. Stoesser D., et al. Development of Lunar Highlands Type Simulants, NU-LHT-1M, -2M. *Geochemica et Cosmochemica Acta*. 72(12):A902.
7. Battler M.M., Spray J.G. The Shawmere Anorthosite and OB1 as Lunar Highland Regolith Simulants. *Planetary and Space Science*. 2009;57(15–15):2128–2131.
8. Gustafson R., White B. Development of a Lunar Dust Simulant. In: *International Conference on Enviornmental Systems Proceedings*. Society of Automotive Engineers; 2009:09ICES-0125.
9. Lunar Soil Characterization Consortium (LSCC). Bidirectional reflectance spectra for lunar soils. Available at: http://www.planetary.brown.edu/relabdocs/LSCCsoil.html.
10. Gaier J.R., Street K.W., Gustafson R.J., Measurement of the Solar Absorptance and Thermal Emittance of Lunar Simulants. *Program*. 2010;(August).
11. 2000 ASTM Standard Extraterrestrial Spectrum Reference E-490-00. 2000. Available at: http://rredc.nrel.gov/solar/spectra/AM0.